

# ROBUSTNESS IN REGULATORY NETWORKS: A MULTI-DISCIPLINARY APPROACH

J. Demongeot<sup>1</sup>, A. Elena<sup>1</sup> and S. Sené<sup>1,2</sup>

<sup>1</sup> TIMC-IMAG, Faculté de Médecine, UJF Grenoble,  
38706 La Tronche, France

<sup>2</sup> LIP, Rhône-Alpes Complex Systems Institute, 5 rue du Vercors,  
69007 Lyon, France

## ABSTRACT

We give in this paper indications about the dynamical impact (as phenotypic changes) coming from the main sources of perturbation in biological regulatory networks. First we define the boundary of the interaction graph expressing the regulations between the main elements of the network (genes, proteins, metabolites,...). Then we search what changes in the state values on the boundary could cause some changes of states in the core of the system (robustness to boundary conditions). After we analyse the role of the mode of updating (sequential, block sequential or parallel) on the asymptotics of the network, essentially on the occurrence of limit cycles (robustness to updating methods). Finally we show the influence of some topological changes (e.g. suppression or addition of interactions) on the dynamical behavior of the system (robustness to topology perturbations).

KEYWORDS: discrete dynamical systems, regulatory networks, cellular automata, robustness.

## 1 INTRODUCTION

The robustness of a regulatory biological (*e.g.* genetic) network is its ability to present no phenotypic change after any modification of the number of its elements (*e.g.* genes) or of their interactions. This property can be provided by an internal redundancy, but, according to Wolfe (Wolfe, 2000), only about 3% of yeast genes with “essential” phenotypes (*i.e.* whose ablation is lethal), compared with about 17% of non-essential yeast genes, are homologues (*i.e.* formed by genome duplication). This suggests that the built-in reliability of genetic networks is not necessarily due to the physical duplication of their components. Many recent works (Borenstein and Ruppin, 2006; Elena *et al.*, 2006; Hornstein and Shomron, 2006) are for example

in favour of a regulation exerted by well conserved RNA “relics” during the evolution, the microRNAs, able to modulate interaction weights of genetic or metabolic regulatory networks. These microRNAs can either keep invariant or, conversely, dramatically change the functional properties of these networks depending on the fact they are active on robust or sensitive parts of their architecture. Because of the more and more important use of the term of robustness in the literature, we think that is of great interest to make more precise this notion. With this paper, our wish is to present a panorama of what we think to be relevant when we speak about robustness in biological systems. For that purpose, we first give some definitions about what is a regulatory network and its associated interaction graph and what we can define as centre and boundary of such a graph. We give then a background information about three main multi-disciplinary views (dependency on boundaries, on updating and on architecture) we can have about robustness in regulatory networks and we finish by a discussion about the ways chosen by real living systems to ensure this robustness.

## 2 PRELIMINARIES

### 2.1 Regulatory networks (Demongeot *et al.*, 2003)

A *regulatory network*  $N$  is made of  $n$  elements (genes, proteins, cells...) and of their interactions. The  $m$  ( $\leq n^2$ ) interactions between these elements are described by an *interaction matrix*  $W$  similar to the synaptic weights matrix which rules the relationships between neurons in a neural network. We denote by  $G$  the *interaction graph* associated to  $W$ , called the incident matrix of  $G$ :  $G$  has a *directed edge* (or arrow) from the  $k^{th}$  element (or *vertex*) of the set  $V$  of vertices of  $N$  to its  $i^{th}$  element, whose weight (or label) equals the coefficient  $w_{ik}$  of  $W$ . If the regulatory network is genetic (we will suppose that it is the case in the following unless an explicit mention), the sign of the coefficient  $w_{ik}$  of  $W$  is equal to  $+1$  (resp.  $-1$ ,  $0$ ) if the gene  $G_k$  activates (resp. inhibits, does not influence) the gene  $G_i$ . If the networks is *boolean*, the *state*  $x_i$  of the gene  $G_i$  is equal to  $+1$  (resp.  $-1$ ) if it is (resp. is not) expressed. The absolute value of  $w_{ik}$  can be any positive real number, but if the interaction mechanism is unknown or difficult to evaluate quantitatively, we choose only the values 1 (if there is an interaction) and 0 (if not).

In order to calculate the  $w_{ik}$  values, we can:

- either determine the *s-directional correlation*  $\rho_{ik}(s)$  between the state vector  $\{x_k(t-s)\}_{t \in C}$  of the gene  $G_k$  at time  $(t-s)$  and the state vector  $\{x_i(t)\}_{t \in C}$  of the gene  $G_i$  at time  $t$ ,  $t$  varying during the cell cycle  $C$  of length  $M = |C|$

and corresponding to observation times of bio-arrays images:

$$\rho_{ik}(s) = \frac{\sum_{t \in C} x_k(t-s) \cdot x_i(t) - \frac{\sum_{t \in C} x_k(t-s) \cdot \sum_{t \in C} x_i(t)}{M}}{M \cdot \sigma_k(s) \cdot \sigma_i(0)}$$

where  $\sigma_k(s) = \left( \frac{M \cdot \sum_{t \in C} x_k(t-s)^2 - (\sum_{t \in C} x_k(t-s))^2}{M^2} \right)^{\frac{1}{2}}$  and then take:

$w_{ik} = \text{sign}\left(\frac{\sum_{s=1}^M \rho_{ik}(s)}{M}\right)$  if  $|w_{ik}| > \eta$ , and  $w_{ik} = 0$  if  $|w_{ik}| \leq \eta$  where  $\eta$  is a de-correlation threshold ;

- or identify the system with a boolean network.

When it is impossible to obtain all the coefficients of  $W$  (neither from the literature nor from such calculations), it is possible to estimate  $W$  by using inverse problem techniques (Aracena and Demongeot, 2004) or to complete  $W$  if it is partially known: we choose randomly the missing coefficients by respecting the *connectivity coefficient*  $K(W) = \frac{I}{N}$ , the ratio between the number  $I$  of interactions and the number  $N$  of genes, and the *mean inhibition index*  $I(W) = \frac{R}{T}$ , where  $R$  is the number of inhibitions.  $K(W)$  is in general between  $\frac{3}{2}$  and 3 and  $I(W)$  between  $\frac{1}{3}$  and  $\frac{2}{3}$ , for many known genetic networks as lactose operon, Cro operon for the phage  $\lambda$ , lysogenic/lytic operon for the phage  $\mu$  (Demongeot *et al.*, 2003), gastrulation network, *Arabidopsis thaliana* flower morphogenesis network (Mendoza and Alvarez-Buylla, 1998)...

## 2.2 Dynamical behaviour of a regulatory network

The regulatory network evolves over time. For example, by basing on the Hopfield model (Hopfield, 1982), the state change of the gene  $G_i$  between times  $t$  and  $t+1$  can obey a *deterministic threshold rule*. Let us define the Hopfield Hamiltonian:  $\mathcal{H}_{\text{Hopfield}}(x_i(t)) = \sum_{k \in \mathcal{N}(i)} w_{ik} \cdot x_k(t) - \theta_i$  where  $\mathcal{N}(i)$  is the neighbourhood of  $i$  in  $G$  and the  $\theta_i$ 's are threshold values. The deterministic threshold rule is then given by  $x_i(t+1) = H(\mathcal{H}_{\text{Hopfield}}(x_i(t)))$  where  $H$  is the sign step function ( $H(y) = 1$  if  $y \geq 0$  and  $H(y) = -1$  if  $y < 0$ ). When time  $t$  increases, the genes states reach a stable set of configurations (fixed configuration or cycle of configurations) called *attractors* of the network dynamics.

The rule can be more generally a *stochastic threshold rule* (we will then speak of stochastic Hopfield model):

$$P(x_i(t+1) = 1) = \frac{e^{\mathcal{H}_{\text{Hopfield}}(x_i(t))/T}}{1 + e^{\mathcal{H}_{\text{Hopfield}}(x_i(t))/T}}$$

We can notice that the stochastic rule becomes the deterministic one when the temperature  $T$  is tending to 0, except for the case where  $\mathcal{H}_{\text{Hopfield}}(x_i(t)) = 0$  where

the probability to have  $x_i(t+1) = 1$  is  $\frac{1}{2}$ . Furthermore, it becomes an equiprobability rule when the temperature is tending to  $+\infty$ .

Let us denote by  $\Gamma^-(i)$  (resp.  $\Gamma^+(i)$ ) the subset of vertices  $\{i_1, i_2, \dots, i_{k(i)}\}$  of  $V$  such that  $(i_j, i)$  (resp.  $(i, i_j)$ ) belongs to the set  $E$  of edges of graph  $G$ , for each  $j = 1, \dots, k(i)$ . We will say that a subset of  $E$ , denoted by  $C = \{e_1, e_2, \dots, e_r\}$  is a *chain* if each  $e_k$  in  $C$  has a vertex belonging to  $e_{k-1}$  and an other one belonging to  $e_{k+1}$ . We will say that  $C$  is *simple* (resp. *elementary*) chain if the edges (resp. vertices) are different. In the sequel, we will understand by chain a simple and elementary chain. In the same way, we will call  $C$  a *path* if  $e_k = (i_k, i_{k+1})$  implies  $e_{k+1} = (i_{k+1}, i_{k+2})$ , for all  $k = 1, \dots, r$ , that is to say the final vertex of each edge is the beginning vertex of the next edge in  $C$ . The sign of a path or a chain  $C$  is positive (equal to  $+1$ ) if the number of negative edges (*i.e.* edges having a negative label) of  $C$  is even and negative (equal to  $-1$ ) if this number is odd. A *circuit* (or *loop*) is defined as a chain (resp. path) where each of the two extremities of any edge belongs to two and only two edges. For simplicity of notation, we will say that a vertex  $i$  belongs to a circuit  $C$  if there exists a node  $j$  such that  $(i, j)$  or  $(j, i)$  belongs to  $C$ . We will call a circuit or loop  $C$  positive (resp. negative) if its sign is positive (resp. negative). We will call *connected component* of  $G$  each set of vertices such that there is a path between every couple of vertices of it along a sequence of edges of  $G$ . A *garden of Eden* is a vertex receiving no edge, but influencing at least one other vertex.

We shall say that  $x$  is a *fixed configuration* if  $x$  is invariant under the application of the complete sequence of updates. If the dynamics of updating leads to the iteration of a finite number of states  $x_i, i = 1, \dots, k$ , then we speak of the cycle  $(x_1, \dots, x_k)$ . The updating iteration mode can be parallel, sequential or block sequential (see section 4.1 for further details). Let us observe that a change in the updating iteration mode does not change the set of fixed configurations, but only changes their attraction basins and may causes the apparition (or the disparition) of cycles of configurations. In the following, we will use systematically the parallel iteration, unless it is specified.

In the sequel, we will recall some important dynamical properties concerning the boolean networks with a deterministic threshold rule (Demongeot *et al.*, 2003). We assume that  $G$  is connected since, otherwise, one can apply the results to each of connected components of  $G$ . In addition, we will suppose with no loss of generality that  $|\Gamma^-(i)| > 0$  for all  $i$  in  $V$  since otherwise, if there exists a vertex  $i$  in  $V$  such that  $\Gamma^-(i)$  is empty, then we can assume that the arc  $(i, i)$  exists in  $E$ . In this way, the dynamics of both networks are the same. It evidently follows from this property that there exists at least one circuit  $C$  in  $G$  (or a circuit of the form  $(i, i)$ ). Finally, we suppose that  $G$  and  $W$  have a quasi-minimal structure, that is to say:  $(j, i)$ , such

as  $i \neq j$ , belongs to  $E$  (or equivalently  $w_{ij} \neq 0$ ), if and only if there exists  $x$  in the state space  $\{-1, 1\}^n$ , such that:

$$\text{sign}(\mathcal{H}_{\text{Hopfield}}(x_i(t))) \neq \text{sign}\left(\sum_{k \in \mathcal{N}(i), k \neq j} w_{ik} \cdot x_k - \theta_i\right)$$

Hence, we have the following necessary condition to have a quasi-minimal structure:

$$\forall i = 1, \dots, n, -\sum_{k=1}^n |w_{ik}| < \theta_i \leq \sum_{k=1}^n |w_{ik}|$$

The next property will be very useful in the following for characterising a positive cycle.

**Proposition 2.1** *A cycle  $C$  is positive if and only if there exists a vector  $x \in \{-1, 1\}^n$  such that for all  $(k, i) \in C$ ,  $\text{sign}(w_{ik}) = x_i \cdot x_k$  or, equivalently, for all  $(k, i) \in C$ ,  $x_i = \text{sign}(w_{ik}) \cdot x_k$ .*

Then we have the following results relating the existence of fixed configurations for  $N$  to the presence of positive or negative circuits (or loops).

**Theorem 2.2** *Given  $N$ , if all circuits of  $G$  are positive, then there exists a vector  $x = (x_1, \dots, x_n) \in \{-1, 1\}^n$  such that  $x$  and  $-x = (-x_1, \dots, -x_n)$  are fixed configurations of  $N$ .*

**Theorem 2.3** *If all circuits of the interaction graph  $G$  are negative, then  $N$  has no fixed points.*

The previous results allow us to characterise some minimal regulatory networks. The following propositions constitute examples of minimal regulatory networks. They solve in part the inverse problem consisting in the description of  $W$  only from the knowledge of a phenotypic  $x$  observed from bio-array images.

**Proposition 2.4** *Let  $N$  be a network composed by  $n$  nodes and  $n$  connections, a necessary and sufficient condition of existence of a fixed configuration  $x$  is the existence of a positive circuit. In this case,  $x$  and  $-x$  are both fixed points. Hence we can characterise the set of minimal  $N$ 's having  $x$  as fixed point.*

**Proposition 2.5** *Given a state vector  $x$ , the set of minimal networks  $N$  having an interaction graph  $G$ , an incident matrix  $W$  and a threshold vector  $\theta$  and having  $x$  as fixed point is given by the following conditions:  $w_{ik} = \alpha_{ik} \cdot x_i \cdot x_k$ , where  $\alpha_{ik} \geq 0$  and, for all  $i$ , there exists  $k(i)$  such that  $\alpha_{ik(i)} \neq 0$ ,  $-|\alpha_{ik(i)}| < \theta_i \leq |\alpha_{ik(i)}|$ .*

**Proposition 2.6** *Let  $N$  be a network composed by  $n$  vertices and  $n+1$  interactions, a necessary and sufficient condition for existence of an attractor of all points parallelly iterated is a negative circuit and a positive circuit intersecting.*

Let  $C$  be a positive circuit of  $N$ , then by Proposition 2.1 above, there exists  $x$  in  $\{-1, 1\}^n$ , such that  $x$  and  $-x$  satisfy the equation:  $(k, i) \in C, \text{sign}(w_{ik}) = x_i \cdot x_k$ . If we denote by  $u(C) \in \{-1, 1\}^n$  the vector defined by  $u(C) = x$  (resp  $-x$ ) if  $x_{i(0)} = 1$  (resp  $-1$ ), where  $i(0) = \min(\{i | i \in C\})$ , then we have the following property:

**Lemma 2.7** *Given a regulatory network  $N$  and  $y$  a fixed configuration of  $N$ , then for all  $i \in V$ , there exists a positive circuit  $C(i)$  in  $G$  such that for all  $k$  in  $C(i)$ ,  $y_k = u(C(i))_k$  or for all  $k$  in  $C(i)$ ,  $y_k = -u(C(i))_k$ .*

**Theorem 2.8** *If  $m$  is the total number of positive circuits of  $N$ , then the number of fixed points of  $N$  is less than or equal to  $2^m$ , and this upper bound is reached if and only if for all circuits  $C$  of  $N$  there does not exist an edge  $(k, i)$  in  $C^C$  ending in  $C$  (there is no garden of Eden  $k$  pending to  $C$ ).*

Let us consider finally a regulatory network  $N$  having  $n$  vertices and  $2n$  interactions such as  $K(W) = 2$ . We search for a mean value of the number of fixed configurations, when  $n$  is growing to infinity.

**Lemma 2.9** *For any graph  $G$  having  $m$  non oriented edges, the mean number of oriented edges we can define on  $G$  from the non oriented topology is equal to  $4m/3$ .*

**Theorem 2.10** *If the regulatory network  $N$  has  $n$  vertices and  $K(W)n$  interactions, with  $K(W) = 2$ , then the expectation of the number of fixed configurations of  $N$  has the same order of magnitude than  $n^{\frac{1}{2}}$ , if  $n$  is sufficiently large.*

We will define now the main features we can associate to the interaction graph  $G$  as equivalent of a centre (or a core) and equivalent of a boundary.

### 2.3 Graphs: centre and boundary (Moore, 1959; Harary, 1969)

A directed graph  $G$  is *regular* if each vertex is the end of the same number of directed edges, *i.e.* every vertex has the same degree or valency. A regular graph with vertices of degree  $k$  is called a *k-regular* graph or regular graph of degree  $k$ . A graph is *planar* if it can be redrawn without intersecting edges. The graph *distance* between  $x$  and  $y$ , distinct vertices of a directed edge-labelled graph, is the minimal sum of the absolute value of the directed edge (or arrow) labels (or weights) among all possible paths between  $x$  and  $y$  (which never repeat a vertex), this sum being called the *length* of the path. The *eccentricity* of a vertex  $x$  is the maximum graph distance between  $x$  and any other vertex of  $G$ . The maximum (resp. minimum

not zero) eccentricity is the graph *diameter* (resp. *radius*). A vertex is *central* if its eccentricity equals the graph radius. The set of all central points is called the graph *centre* (see Figure 1). A vertex is *peripheral* if its eccentricity equals the graph diameter. The set of all peripheral points is called the graph *boundary*. A graph *geodesic* between two vertices  $x$  and  $y$  is any shortest (*i.e.* whose length is the distance between  $x$  and  $y$ ) path between them. The graph *circumference* is the length of any longest circuit (called *perimeter*) of the graph. The graph *girth* is the length of any shortest circuit.

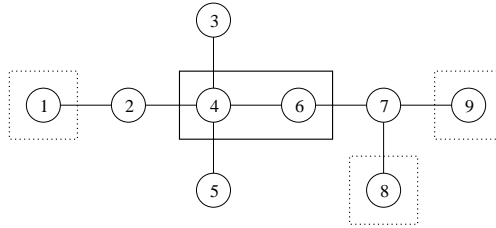


Figure 1: If the label of each arrow of this interaction graph is 1, the diameter is 5, the radius is 3, the centre is the set  $\{4, 6\}$  and the boundary is the set  $\{1, 8, 9\}$ .

If the graph is only undirected and not signed, *e.g.* coming from a non directional (or 0-directional) correlation network, we consider that an edge is bidirected and that it is labelled by the value 1 on each direction. If the graph is directed and signed, *i.e.* if the non zero values of labels are  $+1$  or  $-1$ , depending respectively on the attractive (activator) or repulsive (inhibitor) character of the interactions, then the distance between  $x$  and  $y$  is just the number of arrows of the shortest path going from  $x$  to  $y$ .

In the network which regulates the *Arabidopsis thaliana* flower morphogenesis (Mendoza and Alvarez-Buylla, 1998), the interaction matrix  $W$  is a  $(12, 12)$ -matrix with only 25 non zero labels whose signs are indicated on Figure 2. In this network, it is easy to calculate the diameter, which is equal to 4, as well as the radius, equal to 1. Thus, this network has only a peripheral vertex and four central vertices (see Figure 2).

### 3 ROBUSTNESS TO BOUNDARY CONDITIONS

The dependency on boundary conditions can be expressed in terms of influence exerted on the state values of the centre vertices by the state values of vertices of the boundary in an interaction graph.

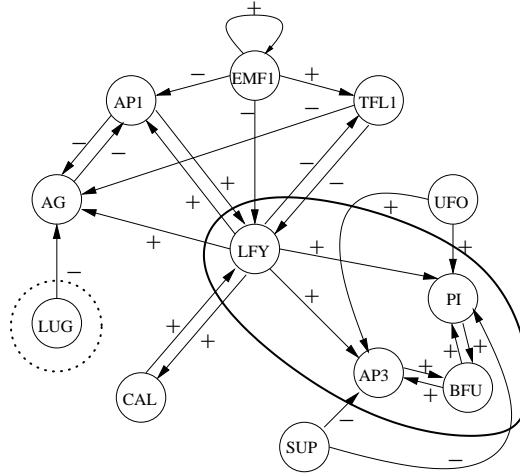


Figure 2: *Arabidopsis thaliana* flower morphogenesis network. If the label of each arrow of this graph is 1, the boundary is delimited by the dotted box and the centre is delimited by the plain box.

### 3.1 Regular planar interaction graph

Let us consider a regular planar interaction graph: the prototype of such a graph has its vertices located on a square in  $\mathbb{Z}^2$  (e.g. the square of side  $n$  centred at the origin of  $\mathbb{Z}^2$ ), see Figure 3. An example is the Ising graph (Ising, 1925) which represents a network of magnetic particles. These particles have two possible states, either up-oriented or down-oriented. The state of a particle is denoted by  $+1$  if it is up-oriented and  $-1$  if it is down-oriented. Furthermore, each vertex of the networks (except those of the boundary) is of degree 4, i.e. for any  $i$  in  $V$ , there are only four neighbours  $j_1, j_2, j_3, j_4$  influencing  $i$  through four directed edges starting in  $j_k$  and ending in  $i$ .

Let us consider the Hamiltonian of the Ising deterministic law:

$$\mathcal{H}_{\text{Ising}}(x_i(t)) = -\left( \sum_{k \in \mathcal{N}(i)} w_{ik} \cdot x_i(t) \cdot x_k(t) - h \cdot x_i(t) \right)$$

The Ising law used for understanding the influence of boundaries is the stochastic version (see Section 2.2) of the threshold rule which is obtained by replacing  $\mathcal{H}_{\text{Hopfield}}$  by  $\mathcal{H}_{\text{Ising}}$ . So, the studied Ising dynamics is quasi-identical to the one presented in section 2.2, with same non zero weights  $w_{ik} = -u_1$  only for the  $k$ 's belonging to the nearest neighbours of  $i$  ( $i$  excluded), where  $u_1$  is the potential of action of a vertex on its nearest neighbours. The threshold  $h \cdot x_i(t) = -u_0$  considered as a constant is called *external field* and the stochastic parameter  $T$  is called *temperature*. The

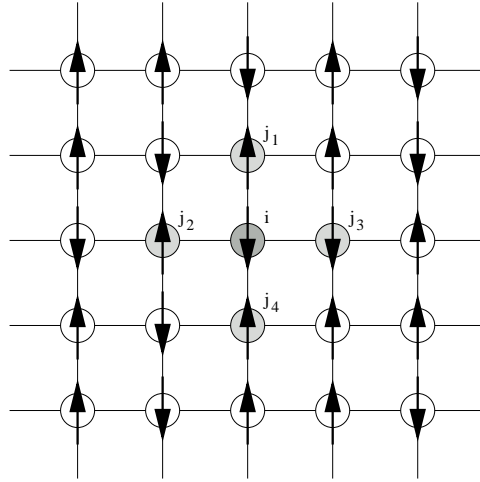


Figure 3: The Ising regular planar interaction graph.

principle is that the state of a vertex has more chance to change if the majority of its neighbours are in the opposite state.

The Ising model has been initially developed for interpreting the ferromagnetism and, further, direct generalisations have been proposed as model for many applications including neural (and more generally regulatory) networks such as the Hopfield model. In the following, we will particularly focus on the stochastic version of this model.

Let us observe that, in the stochastic case, the analogue of a fixed configuration is an invariant measure, *i.e.* a probability distribution invariant during the updating process, called the Boltzmann distribution in the classical isotropic Ising model. This invariant measure is concentrated on fixed configurations, when  $T$  tends to 0.

### 3.2 Irregular planar interaction graph

The known regulatory networks (as the *Arabidopsis* network shown on Figure 2) are in general planar, but not regular. When many relationships between genes of a same functional cluster remain unknown, we can suppose that, in presence of uncertainty, the graph is complete (*i.e.* each ordered pair of graph vertices is connected by a directed edge), all the weights being non zero, but certain having very small absolute value, expressing the probable absence of interaction. These uncertain weights  $w_{ik}$ , if their absolute value belongs to  $[0, 1]$ , can be considered as probabilities of having an interaction between genes  $k$  and  $i$ . If the uncertainty progressively disappears, some weights can vanish and others tend to 1 or  $-1$ . Such graphs can be considered as sub-graphs of an interaction graph, whose they represent

the uncertain part.

### 3.3 Phase transition and emergent behaviours

The phase transition phenomenon we focus on, *i.e.* the dependency of central state values on the boundary state values, has been studied in the attractive case ( $u_1 > 0$ ) of the Ising model by Onsager (Onsager, 1944). He has proved for the planar two-dimensional Ising interaction graph that for certain values of the pair  $(u_0, u_1)$ , located below a certain critical temperature  $T_c$  on a transition line  $u_0 + 2.u_1 = 0$  (see Figure 4), the state value on the centre  $i$  of the graph was highly dependent on the state values on the boundary, when the number of vertices (equal to  $n^2$ , when the side of the Ising square is of length  $n$ ) was tending to infinity. In the repulsive case ( $u_1 < 0$ ), according to Dobrushin and Ruelle (Dobrushin, 1968; Ruelle, 1969), phase transition in the two-dimensional Ising model can be observed in the region of the space  $(u_0, u_1)$  delimited by the two following lines:  $u_0 + 4.u_1 = -\frac{1}{4}$  and  $u_0 = 2$ .

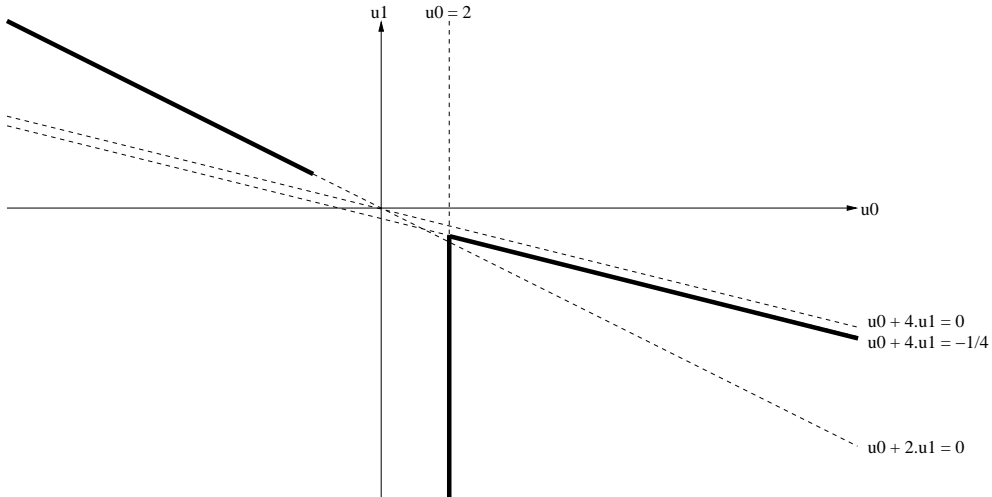


Figure 4: Existence of regions in the parametric plane  $(u_0, u_1)$  in which the transition phase phenomenon occurs, *e.g.* in the attractive case ( $u_1 > 0$ ) at a critical temperature  $T_c$ .

Let suppose now that the lower-left vertex of the interaction graph  $G$  of the Figure 2, the only peripheral vertex belonging to the boundary of  $G$ , is itself regulated by a regular interaction Ising sub-graph, whose it is the centre. If this sub-graph has the number of its vertices tending to infinity, let suppose that the weights are chosen such that a transition phase behaviour occurs. In this case, we can simulate (see Figure 5) the situation of an irregular not planar regulatory network having an uncertain interaction sub-graph of size  $n^2$  controlling a vertex of its boundary, for which if  $n$  is large we have a strong dependency of the centre state values on

the boundary values of the sub-graph. We have in a certain sense transferred the dependency on the boundary state value to the sub-graph boundary.

We will now study some conditions of existence of emergent behaviours in an inhomogeneous Hopfield graph, which could better represent the uncertain part of a regulatory network. The results presented in the following come from simulations of the dynamics of a regular network placed in a squared grid. The size of a side of the square is 64. At the beginning of a simulation, the initial configuration is randomly and independently chosen. The objective is then to compare the influence of different valued boundaries on the network and find the parametric conditions  $(u_0, u_1)$  for which the centre (made of four vertices) of the network is highly dependent on the boundary conditions.

First of all, let us note that we consider the homogeneous stochastic Hopfield model. For the attractive case  $u_1 \geq 0$ , we look at the difference between the probability  $P_1$  to have the state value 1 in the central vertices of the graph knowing that all state values on the boundary are fixed to the value 1, and the probability  $P_{-1}$  to have 1 at the central vertices, knowing that boundary is fixed at  $-1$ . A value significantly different of 0 (at the level 1%) for  $p = |P_1 - P_{-1}|$  is obtained in a neighbourhood of the line  $u_0 + 2.u_1 = 0$ , for  $\frac{|u_0|}{T}$  and  $\frac{u_1}{T}$  more than a strictly positive value, which corresponds to the phase transition phenomenon observed by Onsager (see Figure 6).

For the repulsive case ( $u_1 < 0$ ) (see Figure 7 (left)), we observed a significant space of parametric conditions where the boundaries highly influence the centre for  $|P_{1/-1} - P_{-1/1}|$ , where  $P_{1/-1}$  (resp.  $P_{-1/1}$ ) is the probability to have 1 at the central vertices knowing the left (resp. right) half part of the boundary is fixed at state 1, the other half part being fixed at state  $-1$ . What seems to be relevant is that, despite the neighbourhood of the line  $u_1 \simeq 1$  where an emergent phenomenon occurs, this domain of  $(u_0, u_1)$  is close to the one proposed by Dobrushin delimited by the lines  $u_0 + 4.u_1 = -1/4$  and  $u_0 = 2$  and describing the space of phase transition in a repulsive and homogeneous 2D Ising Model.

In the case of an inhomogeneous Hopfield graph (more realistic for regulatory networks), we used the same technique with a more complex model, where synaptic weights are function of the vertex discrete coordinates. To be more precise, we consider the square  $Q \in \mathbb{Z}^2$ , the relative integers plane, and we define a coordinate system on  $\mathbb{Z}^2$  so that the origin  $O$  belongs to the centre of  $Q$ . Then if  $M_{i,j}$  is the middle in  $R^2$  of both sites  $i$  and  $j$  (with respect to the Manhattan-distance  $d_M$ ), then the synaptic weights are defined as follows:  $w_{ii} = u_0$ ,  $w_{ij} = \frac{u_1}{d_M(M_{i,j}, O)}$  if  $d_M(i, j) = 1$  and  $w_{ij} = 0$  otherwise.

This inhomogeneous stochastic Hopfield model is not translation invariant, but is still a nearest neighbours model. This is interesting and unusual to break the

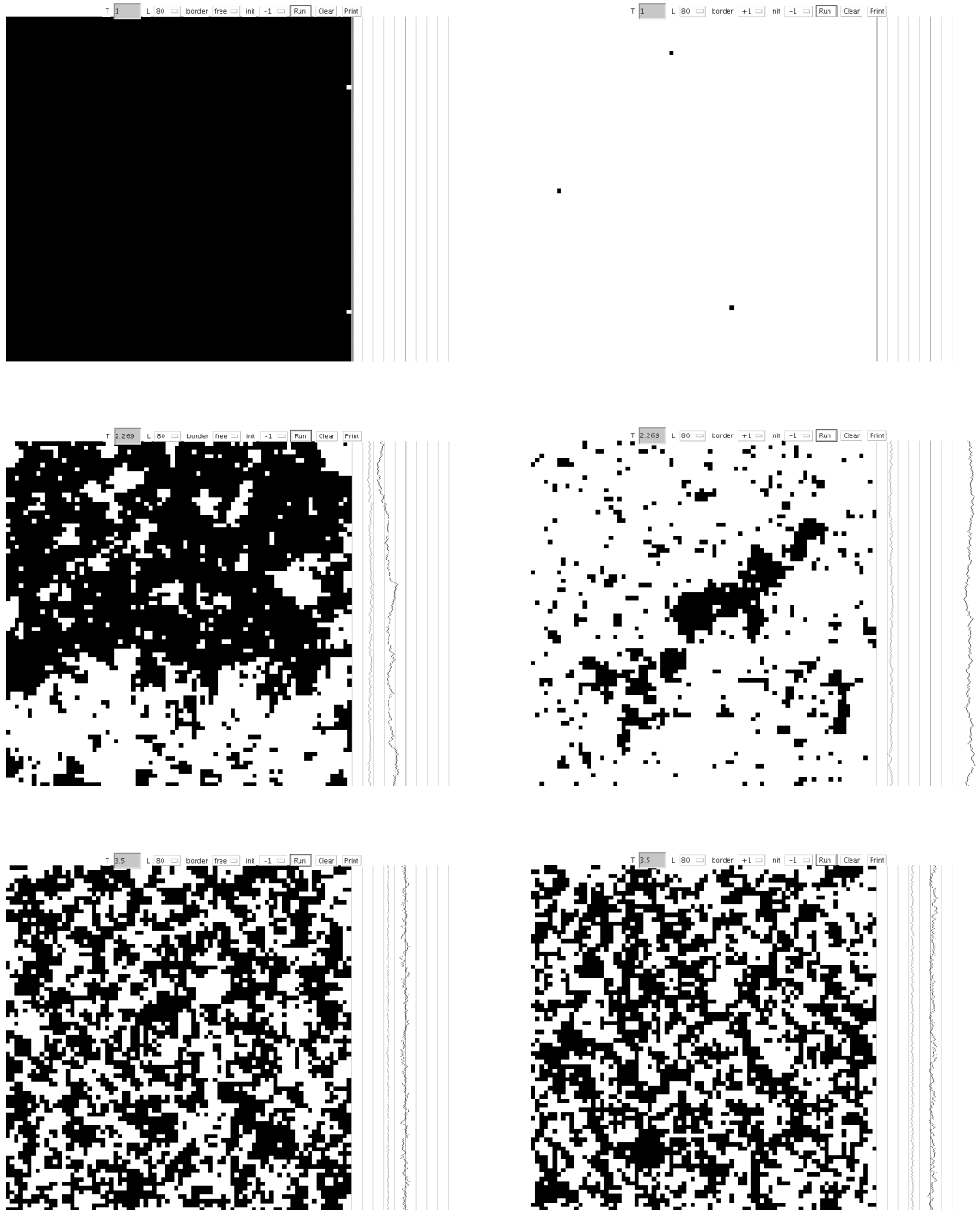


Figure 5: Simulation for  $n = 80$  (using <http://www.ibiblio.org/e-notes/Perc/ising.htm>) of a regular sub-graph in the case of the classical Ising model: vertices in black (resp. white) are in state  $-1$  (resp.  $+1$ ). Different asymptotic behaviours can be observed: dependency on the boundary values at low temperature ( $T = 1$ ), with free boundary (top left) and boundary fixed at  $+1$  (top right); dependency on the boundary values near the critical temperature ( $T = 2.269$ ), with free boundary (middle left) and boundary fixed at  $+1$  (middle right); independency on the boundary values at high temperature ( $T = 3.5$ ), with free boundary (bottom left) and boundary fixed at  $+1$  (bottom right). The black curve on the right of the images corresponds to the evolution of the mean magnetisation  $M$  (mean number of white states  $+1$ ).

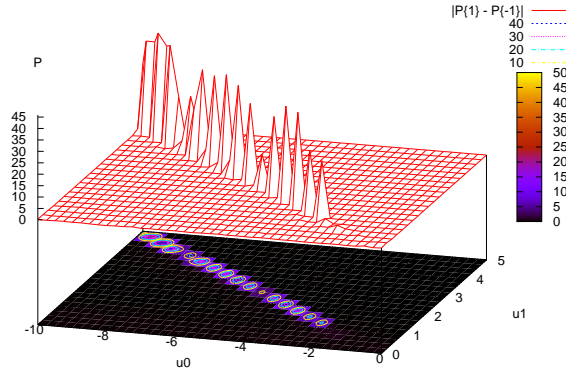


Figure 6: Phase diagram highlighting the existence of a phase transition for the classical and homogeneous Hopfield attractive interaction graphs ( $P$  is given as absolute value of difference of the percentages  $P_1$  and  $P_{-1}$ ;  $u_0$  and  $u_1$  are given in real values).

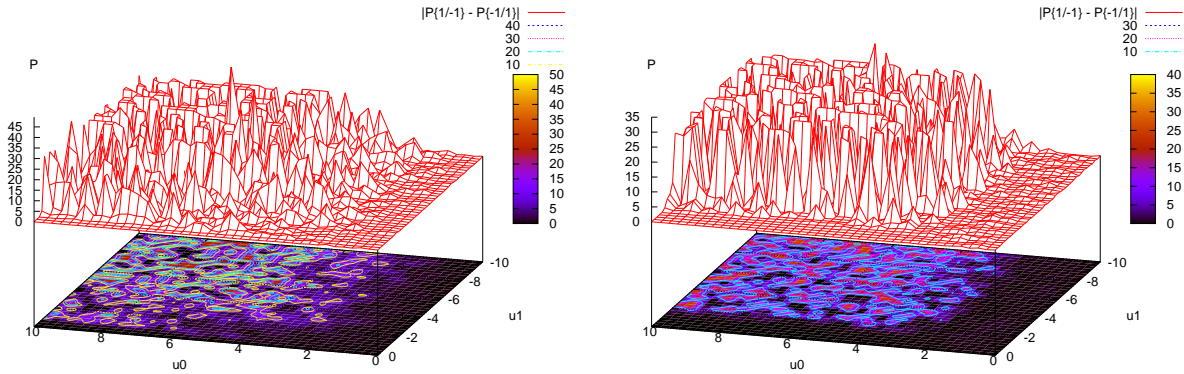


Figure 7: Phase diagram highlighting the existence of a space of parametric conditions for which the centre of the network depends on the boundaries for the classical (left) and inhomogeneous (right) Hopfield repulsive interaction graphs ( $P$  is given as absolute value of difference of the percentages  $P_{1/-1}$  and  $P_{-1/1}$ ).

translation-symmetry, as the majority of phase transition results supposed that the system is translationally invariant, because it is more realistic in the case of regulatory networks. We observe in this case a good significance of the influence of boundaries on the network in a space of parametric conditions (see Figure 7 (right)) which, once again, seems to be very close to the one described by Dobrushin. However, some theoretical studies have to be realized to understand the location of this emergent phenomenon.

Our results show that the phenomenon of influence of boundaries on networks in the stochastic Hopfield model is very close to the results of phase transitions obtained by Onsager for the homogeneous attractive case and to those obtained by Dobrushin for the homogeneous repulsive case. Furthermore, they also give a first answer about what happens when the system is not translationally invariant even if theoretical studies have of course to be developed. Nevertheless, these first simulations seem to be relevant for our purpose because of the nature of regulatory networks. We can notice that in the inhomogeneous case above, the domain of boundary dependence contains still, in the repulsive case, a part of the line  $u_0 + 2.u_1 = 0$  beyond a critical temperature. This line corresponds to the linear dependency between the Bayes conditional equation (giving the probability of states at the centre knowing its boundary) and the projectivity equations (linking the probabilities of states on the boundary), which gives a partial explanation of the boundary dependence (Demongeot, 1981). To finish on this point, it will be now of great interest to prove that these domains of parametric conditions where boundaries influence such networks are phase transitions spaces like for the classical 2D Ising model.

## 4 ROBUSTNESS TO UPDATING METHODS

### 4.1 Robustness to updating iteration modes

The robustness also concerns the dependency of asymptotics on updating iteration modes in the case of deterministic Hopfield model. We will in this section change state space from  $\{-1, 1\}^n$  to  $\{0, 1\}^n$ .

Let  $F : \{0, 1\}^n \rightarrow \{0, 1\}^n$  be a mapping whose components  $f_1, \dots, f_n$  are *threshold functions*:

$$\forall i(1, \dots, n), \forall x \in \{0, 1\}^n, f_i(x) = H(\mathcal{H}_{\text{Hopfield}}(x_i(t)))$$

where  $H$  is defined by  $H(y) = 1$ , if  $y > 0$  and  $H(y) = 0$ , if  $y \leq 0$ .

The *block sequential iteration* on  $F$  associated to the ordered partition  $(I_k)_k$  of the set  $\{1, \dots, n\}$  is defined by:

$$\forall k(1, \dots, p), \forall i \in I_k, x_i(t+1) = f_i(y^k(t))$$

where

$$\begin{cases} y^1(t) = x(t), \\ \forall k(2, \dots, p), y_j^k(t) = \begin{cases} x_j(t+1) & \text{if } j \in I_1 \cup \dots \cup I_{k-1}, \\ x_j(t) & \text{otherwise.} \end{cases} \end{cases}$$

Particular cases of block sequential iterations correspond to particular choices of the partition:

- when the partition is  $(\{k\})_{k=\sigma(1),\dots,\sigma(n)}$  where  $\sigma$  is a permutation of the set  $\{1, \dots, n\}$ , the iteration is called a *sequential* iteration on  $F$ ;
- when the partition is trivially reduced to the unique set  $\{1, \dots, n\}$ , the iteration is called a *parallel* iteration on  $F$ ;

As block sequential iterations on  $F$  can be associated to ordered partitions of the set  $\{1, \dots, n\}$ , one can directly find the number of updating iteration modes for a network composed of  $n$  nodes.

**Proposition 4.1** *Let  $U_n$  be the number of updating iteration modes for a network composed of  $n$  nodes.  $U_n$  satisfies*

$$U_n = \sum_{i=0}^{n-1} \binom{n}{i} U_i \quad \text{where } U_0 = 1.$$

Table 1: Number of updating iteration modes for networks composed by  $n$  nodes.

$n$	1	2	3	4	5	10	12	20
Number of modes	1	3	13	75	541	$1.02 \cdot 10^8$	$2.81 \cdot 10^{10}$	$2.68 \cdot 10^{21}$

Table 1 shows the number of updating iteration modes for some network sizes (numbers of nodes). The number of modes grows exponentially with the size of the network.

As seen in section 2.2, the set of fixed configurations for the network dynamics does not change with the updating iteration mode. Nevertheless, cycles of configurations may appear or disappear if the updating iteration mode changes. In the scope of genetic regulatory networks modeling, fixed points and cycles are very important. Cell types differ because different subsets of genes are "active" in the different cell types. We can then associate each fixed point of the network dynamics to a distinct cell type (Kauffman, 1993, Ch. 12). But there is no evident biological sense to cycles when there are no cyclic behaviour cells.

In the example of the genetic regulatory network for *Arabidopsis thaliana* flower morphogenesis, four (of six) fixed points correspond to the differentiated cells of the flower: stamens, carpels, petals and sepals (Mendoza and Alvarez-Buylla, 1998). The fifth fixed point corresponds to cells that will not become part of flowers, whereas the sixth one does not agree with any observed gene expression pattern in wild-type plants but could be experimentally induced according to the authors. For the network dynamics, the updating iteration mode is based on experimental data: genes are grouped into a hierarchy of five sets depending on their time of activation as the transition to flowering and flower morphogenesis proceeds. The

block sequential iteration corresponds to the following ordered partition of the set  $\{1, \dots, 12\}$ :  $(1, 2)(3, 4, 5)(6, 7, 8)(9, 10, 11)(12)$  (see Figure 8).

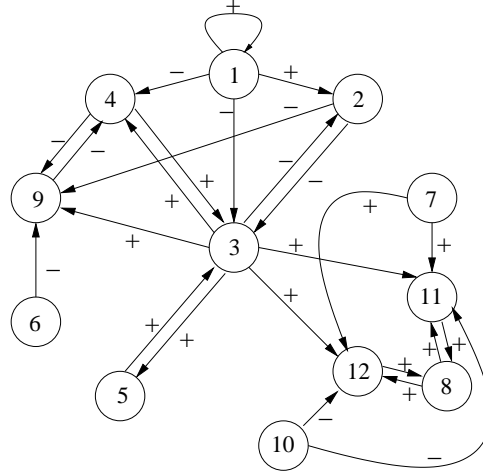


Figure 8: Modified network for *Arabidopsis thaliana* flower morphogenesis.

If the network dynamics is computed with a parallel updating, one observes seven limit cycles of length two and the same six fixed points as with the block sequential updating. These cycles are biologically meaningless. Table 2 refers to the attractors of the *Arabidopsis thaliana* network dynamics depending on the updating iteration mode. Let us notice that genes number 4, 8, 9, 10 and 11 are the only one whose values change in cycles. In the interaction graph, these genes correspond to three (of six) positive circuits of length 2:  $C_1 = \{4, 9\}$ ,  $C_2 = \{8, 10\}$  and  $C_3 = \{8, 11\}$ . These circuits are "broken" in the block sequential updating: vertices belonging to a same circuit are in different groups. Because of the huge number of updating iteration modes for a network composed by twelve nodes (see Table 1) and because the execution time exponentially grows with network size, we have not computed every possible dynamics for the genetic regulatory network for *Arabidopsis thaliana* flower morphogenesis. However, this biological example shows that robustness also concerns the dependency of asymptotics on updating iteration modes.

As every trajectory in the dynamics of a network composed by  $n$  nodes is ultimately periodic (ending to a fixed point or a cycle) whatever the updating iteration mode is, we can define four classes of dynamic behaviour for regulation networks:

- $B_1$ : whatever the updating iteration mode is, every trajectory ends to a fixed point;
- $B_2$ : whatever the updating iteration mode is, every trajectory ends to a cycle;

Table 2: Attractors of the *Arabidopsis thaliana* network dynamics for the biologically inspired block sequential iteration and for the parallel iteration, and the corresponding cell types.

Attractors	Block sequential updating	Parallel updating	Cell types
Fixed point 1	000100000000	000100000000	Sepal
Fixed point 2	000100010110	000100010110	Petal
Fixed point 3	000000001000	000000001000	Carpel
Fixed point 4	000000011110	000000011110	Stamen
Fixed point 5	110000000000	110000000000	No flower
Fixed point 6	110000010110	110000010110	Mutant
Cycle 1	None	000100010000 000100000110	None
Cycle 2	None	000000000000 000100001000	None
Cycle 3	None	000000010000 000100001110	None
Cycle 4	None	000000000110 000100011000	None
Cycle 5	None	000000010110 000100011110	None
Cycle 6	None	000000001110 000000011000	None
Cycle 7	None	110000000110 110000010000	None

- $B_3$ : whatever the updating iteration mode is, some trajectories end to a fixed point, others to a cycle;
- $B_4$ : depending on the updating iteration mode, either every trajectory ends to a fixed point or some trajectories end to a fixed point, others to a cycle.

$B_1$ ,  $B_2$  and  $B_3$  correspond to regulation networks that are robust to updating iteration modes, while  $B_4$  corresponds to networks that are sensitive to updating iteration modes, like the *Arabidopsis thaliana* one.

Our aim is to understand what makes networks behave differently, and in the case of  $B_4$ -class networks, what the relationship between block sequential iterations and asymptotic configurations (fixed points or cycles) is. Previous studies (Goles *et al.*, 1985; Goles and Martinez, 1990; Cosnard and Goles, 1997) have shown that

networks with symmetric matrices and non negative diagonals are  $B_1$  class networks. This result has even been generalized for quasi-symmetric matrices. But this class of interaction matrices is not relevant from a biological point of view when modelling regulation networks.

We have done some simulations on little size networks. We have worked on networks with two and three nodes and on null-threshold functions. Interaction weights were chosen in  $\{-1, 0, 1\}$ . Let us notice that within these conditions there is no network belonging to the  $B_2$  class because the null configuration is always a fixed configuration. Table 3 shows the total number of simulated networks, and the number of networks belonging to each class.

Table 3: Numbers of simulated networks for each size.

Size	Total	$B_1$	$B_2$	$B_3$	$B_4$
2	81	73	0	4	4
3	19683	14818	0	2241	2624

Each one of the four networks composed by two nodes that are belonging to the  $B_4$  class comprises a positive circuit  $C = \{1, 2\}$  (both edges are positive) as shown in Figure 9. Block sequential iterations that break this circuit (sequential iterations in this case) allow only fixed points while the parallel iteration allow cycles and fixed points. Thus the dynamic behaviour of these two-nodes networks is very similar to that observed for the *Arabidospis* network.

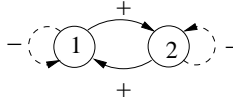


Figure 9: Interaction graph for the 4  $B_4$ -class networks of size two. Edges that are present in each network are in solid lines. Edges that are only present in some networks are in dashed lines.

The network whose interaction graph is represented in Figure 10 is also a  $B_4$ -class network. It is composed of three nodes and its dynamic behaviour is not similar. Fixed points are observed for the following block sequential iterations: (1)(3)(2), (2)(1)(3), (3)(2)(1), (1, 3)(2) and (2)(1, 3). For the eight other iterations trajectories end to fixed points and cycles. The (1)(2)(3) block sequential iteration breaks the positive circuit of length three of the graph as other sequential iterations but allows cycles. In this example, there is no direct link between positive circuits of the interaction graph and blocks that allow only fixed points.

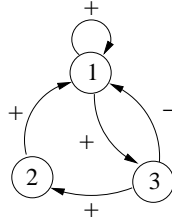


Figure 10: Interaction graph of one of the 2624  $B_4$ -class networks with three nodes.

Our very simple examples show that the link between the interaction graph and the dynamic behaviour of a network is not straightforward. It is important to notice that all regulation networks are not robust to updating iteration modes.

## 4.2 Robustness and asynchronous cellular automata

Cellular automata were originally introduced by von Neumann to study the logical properties of self-reproducing and self-organising machines. Their study is attractive for biology because of their general properties which seem sometimes to be close to those of living systems.

However, the classical researches about this model have been based on specific features and very strong hypotheses about the network and its transitions that seem to be too far from the reality of living systems. Indeed, cellular automata have been essentially studied with perfect synchrony on regular lattices. Recent researches about the robustness to asynchronism of cellular automata have given new relevant results, that have more chance to be close to the reality of biological systems. These researches have mainly focused on the case where perturbations of synchrony are added. They have brought to classify elementary cellular automata in four experimental classes of robustness. In this subsection, we will briefly present the results obtained on this subject (Fatès, 2004; Fatès and Morvan, 2005).

**Definition 4.2** *An asynchronous cellular automaton is a 5-tuple  $(\mathcal{L}, \mathcal{Q}, G, f, \Delta)$  such as: i) a cell is a variable that takes its values in  $\mathcal{Q}$  which is the set of possible states; ii) the set of all cells is called the lattice, denoted by  $\mathcal{L}, \mathcal{L} \subseteq \mathbb{Z}^d$  where  $d$  is the dimension of the lattice; iii) the neighbourhood of a cell  $N(c)$  is a function that associates to a cell  $c$  an ordered set of cells. The cardinality of  $N(c)$  is constant and is equal to  $N$ ; iv)  $f : \mathcal{Q}^n \rightarrow \mathcal{Q}$  is the local transition rule that defines how the new state of a cell  $c$  is computed. This computation is function of the states of the cells belonging to the neighbourhood of  $c$ ; v)  $\Delta : \mathbb{N} \rightarrow \mathcal{P}(\mathcal{L})$  is the updating method which defines for each time  $t$ , the set of cells to which the transition rule is applied.*

We can denote by  $\Delta_\alpha$  the *asynchronous stochastic dynamics* defined by assigning

at each time  $t$  to every cell  $c \in \mathcal{L}$  a probability  $\alpha$  which corresponds to the probability this cell  $c$  is in  $\Delta(t)$ .  $\alpha$  is called the *synchrony rate*. Moreover, we call *configuration* at time  $t$ , which is denoted by  $x_t = (x_t(c))_{c \in \mathcal{L}}$  with  $x \in \mathcal{Q}^{\mathcal{L}}$ , an assignment of a state to each cell of  $\mathcal{L}$ . Thus, when  $\Delta$  is fixed, the global transition function  $F_{\Delta} : \mathcal{Q}^{\mathcal{L}} \times \mathbb{N} \rightarrow \mathcal{Q}^{\mathcal{L}}$  which associates to the configuration at time  $t$   $x_t = (x_t(c))_{c \in \mathcal{L}}$  the configuration at time  $t + 1$   $x_{t+1} = (x_{t+1}(c))_{c \in \mathcal{L}}$  such that:

$$x_{t+1}(c) = \begin{cases} f(N(c)) & \text{if } c \in \Delta(t), \\ x_t(c) & \text{otherwise.} \end{cases}$$

Our aim is here to show on examples that the asynchrony may lead to instabilities that can bring to the emergence of new behaviours. However, we have to notice that the influence of asynchrony depends on the nature of the automaton and that it can easily be highlighted by simulations (all the simulations presented here have been obtained by using FiatLux – <http://nazim.fates.free.fr/Logiciel.htm>).

For our purpose, we give two examples of simulations of asynchrony on 1D cellular automata, the first one showing an important dependence on the synchrony rate and the second one being  $\alpha$ -invariant (*i.e.* its behaviour does not significantly change with the synchrony rate). The cellular automaton of Figure 11 is  $\alpha$ -dependent, *i.e.* its behaviour significantly changes with the synchrony rate, in particular just near a critical value  $\alpha_c$  where a phase transition can be observed. When  $\alpha > \alpha_c$  (*e.g.*  $\alpha = 0.75$ ), the space-time diagrams illustrates branching structures whereas when  $\alpha < \alpha_c$  (*e.g.*  $\alpha = 0.5$ ), those branching structures quickly dies to become a fixed point only composed of cells at state 0.



Figure 11: Simulation of the evolution of the  $\alpha$ -dependent elementary cellular automata 50: (left)  $\alpha = 1.0$  (centre)  $\alpha = 0.75$  (right)  $\alpha = 0.5$ . The critical value of  $\alpha$  for this automaton is approximately  $\alpha_c = 0.63$ .

The cellular automaton of Figure 12 is a version of the “majority vote rule” (*i.e.* the next state of a cell is the most represented state of the cells of its neighbourhood) and is  $\alpha$ -invariant. The behaviour of this automaton depends on the initial density but is invariant relatively to the synchrony rate.



Figure 12: Simulation of the evolution of the  $\alpha$ -invariant elementary cellular automata 232: (left)  $\alpha = 1.0$  (centre)  $\alpha = 0.75$  (right)  $\alpha = 0.5$ .

The two examples given in Figure 11 and Figure 12 above belong to two of the four classes of robustness defined in (Fatès and Morvan, 2005). An interesting point coming from this study is that those empirical classes of robustness cannot be directly deduced from Wolfram’s empirical classification (Wolfram, 1984). Cellular automata are here differentiated thanks to the density parameter. So, it could be of great interest to study the density in regulation networks too. Moreover, as regulation networks do not evolve with a perfect synchrony, we think that a generalisation of this study to graphs having the properties of genetic regulatory networks could lead to a significant advance in understanding the dynamics of these networks.

## 5 ROBUSTNESS TO TOPOLOGY PERTURBATIONS

### 5.1 Topology perturbation on asynchronous *game of life*

The *game of life* is a very famous cellular automaton devised by J. H. Conway in 1970 (Conway, 1970) which has been proved to be computation universal (Durand and Róka, 1998). In this subsection, after a brief description of this model, we will present the results obtained in (Fatès and Morvan, 2004). This paper shows that the structure of the game of life is not stable against synchrony variation. The authors examine what happens when topology perturbations are introduced. They observe that the introduction of such perturbations makes the system more robust to asynchrony.

The game of life is a 2D cellular automata run on a regular subset of  $\mathbb{Z}^2$  where the neighbourhood of each cell is the Moore neighbourhood (*i.e.* the 8 nearest neighbours). Furthermore, as it is shown in (Blok and Bergersen, 1997), the role of the type of boundary conditions is important. Here, we consider a finite grid. At each time step, the following effects occur: (i) any living cell with fewer than two living neighbours dies, as if by loneliness, (ii) any living cell with more than three



Figure 13: Simulation of the evolution of the game of life: (left)  $\alpha = 1.0$  (centre)  $\alpha = 0.75$  (right)  $\alpha = 0.5$ .

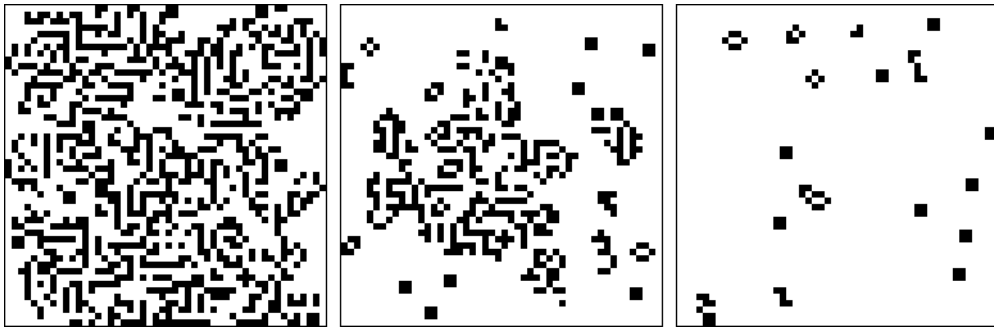


Figure 14: Simulation of the increasing of the robustness to asynchrony of the game of life by perturbing the topology when the synchrony rate is  $\alpha = 0.5$ : (left)  $\epsilon^- = 0$  (centre)  $\epsilon^- = 0.05$  (right)  $\epsilon^- = 0.1$ .

living neighbours dies, as if by overcrowding, (iii) any living cell with two or three living neighbours lives and (iv) any dead cell with exactly three neighbours comes to life.

The game of life is strongly sensitive to asynchrony. Indeed, we can succeed in changing its behaviour by adding asynchrony. Figure 13 is an illustration of this phenomenon which highlights a labyrinthine structure when the synchrony rate decreases.

However, it is possible to increase the robustness to asynchrony of the game of life by perturbing the topology of the network. The choice made here is to balance the instability due to a dynamical property, the decrease of the synchrony rate, with a static property, which is here the definitive removal of a percentage of links. This process is of great biological interest because the aim of this work is to know how



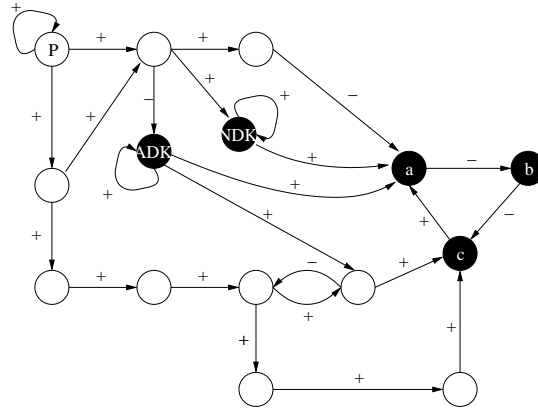


Figure 16: Identification of the peripheral vertex  $P$  of the gastrulation graph  $G$ , and of its central vertices  $a$ ,  $b$ ,  $c$ .

a key cell for gastrulation, the bottle cell. The overall effect of NDKs is to transfer a phosphate group from a nucleoside triphosphate to a nucleoside diphosphate. Starting with adenosine triphosphate (ATP) and guanosine diphosphate (GDP), the action of NDK would produce adenosine diphosphate (ADP) and guanosine triphosphate (GTP):  $ATP + GDP \rightleftharpoons ADP + GTP$ . The interaction graph  $G$  has four fixed configurations, if we use the deterministic majority rule (all weights have the same absolute value 1). One corresponds to the states values  $+1$  for  $P$ ,  $-1$  for ADK,  $+1$  for NDK,  $+1$  for the others except  $+1$ ,  $-1$ ,  $+1$  for the central genes  $a$ ,  $b$ ,  $c$  (see Figure 16). The three other fixed configurations correspond to: i)  $x_P(\infty) = -1$ , like all other genes, ii)  $x_P(\infty) = -1$ , like all other genes except  $x_{NDK}(\infty) = +1$  and  $x_a(\infty) = +1$ , iii)  $x_P(\infty) = -1$ , like all other genes, except  $x_{ADK}(\infty) = +1$  and  $x_a(\infty) = +1$ , iv)  $x_P(\infty) = -1$ , like all other genes except  $x_{ADK}(\infty) = x_{NDK}(\infty) = +1$  and  $x_a(\infty) = +1$ .

If we consider now the original graph  $G$  proposed by M. Leptin (see Figure 17) and if we use the deterministic majority rule, there is only two fixed configurations for this original graph  $G$ : if the gene  $P$  is on (its state value equals  $+1$ ) then the state values of the central genes  $a$ ,  $b$ ,  $c$  equal respectively  $+1$ ,  $-1$ ,  $+1$ , whereas when  $P$  is off (value  $-1$ ), they are  $-1$ ,  $-1$ ,  $-1$ .

## 6 DISCUSSION

It is in general of a great biological interest and relevance to determine the incident matrix  $W$  of an interaction graph  $G$  expressing the relationships between genes, or proteins, or metabolites, or neurons,... This matrix can be inferred from the raw data, but  $W$  is often noisy and/or partially known due to both uncertainty



of robustness of the matrix  $W$  too sensitive to architecture/updating/boundary variations and in case of a lack of observability of its attractors,  $W$  has some chance to be very incorrect, because the architecture of  $W$  is often the result of a long evolution and probably the nature has selected robust (to environmental perturbations) solutions for the regulation (especially if the function controlled by  $G$  is vital). More, if the phenomenology does not give access to all the attractors by varying experimental conditions, it signifies that certain attractors are difficult to be observed, in other terms there exist rare modes of dynamical expression and Maupertuis principle excludes in general such rare dynamics involving in general superfluous interactions. The remarks above justify the interest to revisit the incident matrices of known interaction graphs in order to detect pathologic situations of lack of robustness or of non-observability of attractors (*e.g.* attractors having a small attraction basin, that is presenting few initial conditions leading asymptotically to themselves). If we have to choose a pertinent matrix  $W$  inside a set of possible, we have to privilege the most robust ones having as attractors those which have been really observed, and to leave far away the non robust matrices having more a lot of artefactual asymptotic dynamical behaviours. That justifies the chosen approach and pushes to continue to explore the parametric domains where a small perturbation in the architecture/updating/boundary parameters values causes a big change in the number and nature of attractors ("infrastructural" bifurcation). This domain of study could be called infrastructural instabilities analysis, the adjective "infrastructural" referring to the specific character of the concerned parameters, involved in defining the architecture, the mode of updating and/or the boundary conditions of the interaction graphs and their associated incident matrices.

## 7 CONCLUSION

We have described in this paper different situations of infrastructural instability for incident matrices of interaction graphs in various biological regulatory systems. This first approach shows that certain matrices are highly sensitive to environmental and/or experimental modifications that could affect the number of elements in interaction, or the number of these interactions, or their nature (inhibitory or activatory), or the states of some elements depending on experimental protocols and/or on external physico-chemical conditions (boundary elements), or the temporality (synchrony or asynchrony) of the dynamics of states changes of the (observed or hidden) elements. The present study is preliminary and it is concerned by numerous parallel works about the robustness of specific or generic regulatory networks. An interesting perspective is now the elucidation of the ways in which the nature has selected robust regulatory mechanisms and we will see in the future the explicitation of functional phylogenetic trees showing filiations of parameter sets defining interaction graphs and incident matrices. The analysis of these trees will probably

show situations of high robustness and infrastructural stability and lead to a set of "optimal" or "viable" interaction graphs minimizing environmental influences on their dynamical properties. The way to reach this optimality or viability through the evolution could constitute a real challenge for future studies in comparative physiology or genomics.

## REFERENCES

- Aracena, J. and J. Demongeot (2004). Mathematical methods for inferring regulatory networks interactions: application to genetic regulation. *Acta Biotheoretica* 52: 391-400.
- Aracena, J., M. Gonzalez, A. Zuniga, M.A. Mendez and V. Cambiazo (2006). Regulatory network for cell shape changes during *Drosophila* ventral furrow formation. *Journal of Theoretical Biology* 239: 49-62.
- Blok, H.J. and B. Bergersen (1997). Effect of boundary conditions on scaling in the "game of life". *Physical Review E* 55: 6249-6252.
- Borenstein, E. and E. Ruppin (2006). Direct evolution of genetic robustness in microRNA. *Proceedings of the National Academy of Sciences of the United States of America* 103: 6593-6598.
- Conway, J.H. (1970). The game of life. *Scientific American*.
- Cosnard, M. and E. Goles (1997). Discrete State Neural Networks and Energies. *Neural Networks* 10: 327-334.
- Demongeot, J. (1981). Asymptotic inference for Markov random field on  $\mathbb{Z}^2$ . *Numerical Methods in the Study of Critical Phenomena, Springer Series in Synergetics* 9: 254-267.
- Demongeot, J., J. Aracena, F. Thuderoz, T.P. Baum and O. Cohen (2003). Genetic regulation networks: circuits, regulons and attractors. *Comptes Rendus de l'Académie des Sciences Biologies* 326: 171-188.
- Dobrushin, R.L. (1968). The problem of uniqueness of a Gibbsian random field and the problem of phase transitions. *Functionnal Analysis and Its Application* 2: 302-312.
- Durand, B. and Z. Róka (1998). The game of life: universality (revisited). *École normale supérieure de Lyon Research Report #98-01*.
- Elena, S.F., P. Carrasco, J.A. Daros and R. Sanjuan (2006). Mechanisms of genetic robustness in RNA viruses. *EMBO Reports* 7: 168-173.
- Fatès, N. and M. Morvan (2004). Perturbing the topology of the game of life increases its robustness to asynchrony. *Lecture Notes in Computer Science Proceedings of 6th International Conference on Cellular Automata for Research and Industry*

(ACRI'04) 3305: 111-120.

Fatès, N. (2004) Robustesse de la dynamique des systèmes discrets : le cas de l'asynchronisme dans les automates cellulaires. École normale supérieure de Lyon Thesis.

Fatès, N. and M. Morvan (2005). An experimental study of robustness to asynchronism for elementary cellular automata. *Complex Systems* 16: 1-27.

Goles, E. and S. Martinez (1990). Neural and automata networks: dynamical behavior and applications. *Mathematics and its Applications* 58. Kluwer Academic Publishers, Boston.

Goles, E., F. Fogelman-Soulié and D. Pellegrin (1985). Decreasing energy functions as a tool for studying threshold networks. *Discrete Applied Mathematics* 12: 261-277.

Harary, F. (1969). *Graph theory*. Addison-Wesley.

Hopfield, J.J. (1982). Neural networks and physical systems with emergent collective computational abilities. *Proceedings of the National Academy of Sciences of the United States of America* 79: 2254-2558.

Hornstein, E. and N. Shomron (2006). Canalization of development by microRNAs. *Nature Genetics* 38: S20-S24.

Ising, E. (1925). Beitrag zur theorie des ferromagnetismus. *Zeitschrift fur Physics* 31: 253-258.

Kauffman, S.A. (1993). *The Origins of Order: Self-Organization and Selection in Evolution*. Oxford University Press, Oxford.

Leptin, M. (1999). Gastrulation in *Drosophila*: the logic and the cellular mechanisms. *EMBO Journal* 15: 3187-3192.

Leptin, M. (2005). Gastrulation movements: the logic and the nuts and bolts. *Development Cell* 8: 305-320.

Mendoza, L. and E.R. Alvarez-Buylla (1998). Dynamics of the genetic regulatory network for *Arabidopsis Thaliana* flower morphogenesis. *Journal of Theoretical Biology* 193: 307-319.

Moore, E. (1959). Shortest path through a maze. *Annals of Computation Laboratory of Harvard University* 30: 285-292.

Onsager, L. (1944). Crystal statistics. I. A two-dimensional model with an order-disorder transition. *Physics Review* 65: 117-149.

Ruelle, D. (1969). *Statistical mechanics, rigorous results*. World Scientific, Imperial College Press.

Wolfe, K. (2000). Robustness - it's not where you think it is. *Nature Genetics* 25:

3-4.

Wolfram, S. (1984) Universality and complexity in cellular automata. *Physica D: Non Linear Phenomena* 10: 1-35.